

Electronic structure and magnetism of the semimetals ErAs and $\text{Er}_x\text{Sc}_{1-x}\text{As}$

A. G. Petukhov, W. R. L. Lambrecht, and B. Segall

Department of Physics, Case Western Reserve University, Cleveland, Ohio 44106-7079

(Received 23 May 1994)

We present results of linear muffin-tin-orbital band-structure calculations of ErAs in the local-spin-density approximation. While the exchange splitting and cyclotron masses are in good agreement with experimental data, we find the Fermi surface dimensions of this semimetal to be significantly overestimated. A good fit to recently measured Shubnikov-de Haas oscillations in $\text{Er}_x\text{Sc}_{1-x}\text{As}$ is obtained when the Δ'_2 band is shifted upward by a quasiparticle self-energy correction. The effects due to alloying with Sc are taken into account in a virtual-crystal approximation.

Palmstrøm *et al.*^{1,2} recently reported heteroepitaxial growth of semimetallic rare-earth (RE) monoarsenides ErAs and $\text{Er}_x\text{Sc}_{1-x}\text{As}$ on GaAs, and vice versa, and thus opened the way towards the development of a metal-base transistor made from these materials. The interesting magnetic properties of ErAs ,³ which is an antiferromagnetic semimetal with magnetism induced by the open $4f$ shell, add further interest to this system. Magnetotransport investigations of thin epitaxial films of $\text{Er}_x\text{Sc}_{1-x}\text{As}$ and ErAs buried in GaAs were reported by Allen *et al.*⁴ and Bogaerts *et al.*⁵ and provide important experimental information on the band structure. The interpretation of these results was based on Hasegawa and Yanase's calculations⁶ for GdAs, the only previous first-principles band structure calculation available for RE arsenides. Those calculations were non-spin-polarized and were restricted to the experimental lattice constant. Here, we report spin-polarized calculations of ErAs , including total energy properties as a function of lattice constant. In addition, we make a detailed comparison with the experimental data on the Fermi surface of ErAs and $\text{Er}_x\text{Sc}_{1-x}\text{As}$. Our results provide several insights into the electronic structure of these materials. Our main finding is that the Fermi-surface dimensions are significantly overestimated by the local-density approximation. Using a semiempirical quasiparticle self-energy correction, however, excellent agreement is obtained with Shubnikov-de Haas (SdH) oscillations.⁵ Our results also have consequences for the question of whether or not size quantization in ultrathin layers will turn these semimetals into semiconductors.^{2,7}

The computational method employed in this work is

the density functional theory⁸ in the local-spin-density approximation (LSDA).⁹ The scalar-relativistic linear muffin-tin orbital (LMTO) method¹⁰ is used in the atomic-sphere approximation (ASA) including empty spheres in the interstitial region and both the combined correction term and the muffin-tin or Ewald correction.¹¹ Since the localized spins of $4f$ electrons in rare-earth compounds are very well established even above the Néel temperature,⁴ we treat them self-consistently as outer core electrons with both $4f$ spin-up and spin-down occupation numbers fixed. That means that the $4f$ electrons are not allowed to hybridize with s , p , and d valence electrons.¹² This *constrained* local-spin-density functional approach¹³ is close to that used by Hasegawa and Yanase⁶ for GdAs and by Brooks *et al.*¹⁴ in their treatment of rare-earth-transition-metal compounds. For simplicity, our spin-polarized calculations are carried out for the ferromagnetic instead of the antiferromagnetic alignment of the spins. This should have minor consequences for the magnitude of the induced moments and their orientation with respect to that of the $4f$. The ferromagnetic spin-polarized band structures represent the saturation limit of the paramagnetic state in a strong magnetic field (saturation field ~ 4 T). The non-spin-polarized calculation can be thought of as a virtual-crystal approximation for the situation of randomly oriented $4f$ moments.¹⁵

Our results for ground-state properties of ErAs are presented in Table I. The optimum valency for erbium is found to be $\text{Er}^{3+}(4f^{11})$ by calculating the total energy for various $4f$ occupations. In this configuration, the three valence electrons most efficiently share the valence

TABLE I. Equilibrium lattice constants a (in Å), cohesive energies E_{coh} (in eV/atom) in paramagnetic (P) and ferromagnetic (F) phases, bulk modulus (in GPa), and magnetic moments (in μ_B per unit cell) of ErAs .

a , theor. (expt.) ^a	E_{coh} ^b (P , F)	B	μ_{Er}	μ_{As}	μ_{tot}
5.70 (5.73)	3.172, 3.174	93.70	0.036	-0.027	0.008

^aReference 3.

^bCohesive energy (eV/atom) with respect to neutral atoms in their spin-polarized LDA ground state, including $4f$ spin polarization in all cases.

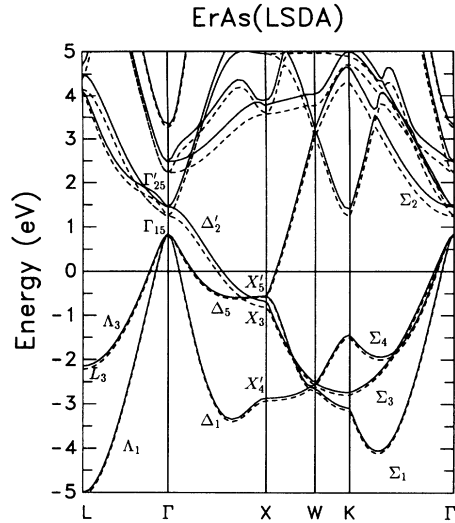


FIG. 1. Electronic band structure of ErAs (ferromagnetic phase) in the local-spin-density approximation. The solid (dashed) curves are for the spin-down (-up) bands with up denoting the direction of the $4f$ spins.

bands with the five As electrons in mainly As $4s$ and As $4p$ derived bands. The latter, however, are hybridized with the Er $5d$ bands, one of which (the Δ'_2 band) dips below the As $4p$ band at X . This leads to a semimetallic state. The lattice constant is in good agreement with experiment. The cohesive energy in the ferromagnetic state and the paramagnetic state differ by only 2 meV/atom when, as indicated above, the $4f$ contribution of 1.74 eV to the spin-polarization energy is assumed to remain present in the paramagnetic phase. This nearly vanishing energy difference is consistent with the low Néel temperature ($T_N = 4.5$ K).⁴ The valence-electron contributions to the magnetic moments induced by the Er $4f$ on Er and As atoms are significant, but they nearly cancel each other. The Er $5d$ moment is parallel to the Er $4f$ moment in accordance with Hund's rules.

The spin-polarized band structure of ErAs is shown in Fig. 1. The overall picture is quite similar to that for GdAs obtained by Hasegawa and Yanase in their non-spin-polarized calculations.⁶ The Fermi surface consists of one light- and two heavy-hole sections near Γ and three electron pockets at the equivalent X points. These are shown in Fig. 2 for the non-spin-polarized band structure. As expected, the exchange splitting of the mainly Er-derived conduction bands is significantly larger than that of the mainly As-derived valence bands.

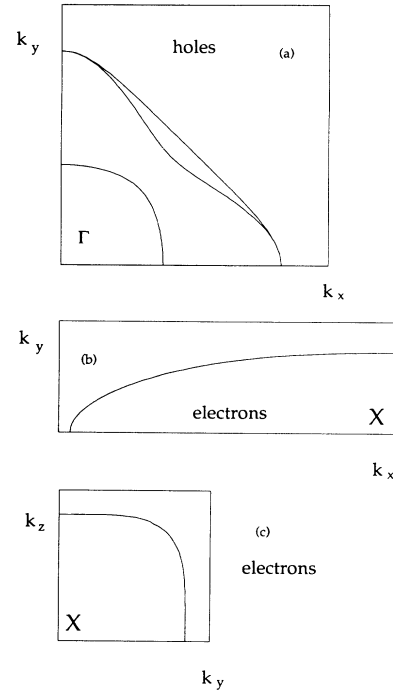


FIG. 2. Cross sections of the LDA Fermi surfaces of ErAs (in the paramagnetic phase) for (a) holes and (b), (c) electrons; (b) shows the longitudinal cross section in the Γ - X - W plane with $k_x = k_{\parallel}$, and (c) shows the transverse cross section in the U - X - W plane with both k_y and k_z along equivalent X - W directions.

The exchange splitting at the Fermi level is also strongly anisotropic due to the different weights of the Er and the As contributions in the bands along the Δ (Γ - X) and Z (X - W) axes. The calculated transverse splitting $\Delta_{\perp} = 80$ meV is in good agreement with the 64–81 meV range of values deduced from beatings in the SdH oscillations observed by Allen *et al.*⁴ and Bogaerts *et al.*⁵ The longitudinal splitting Δ_{\parallel} is calculated to be 157 meV. Here and in the following discussion of SdH frequencies and masses, longitudinal (\parallel) refers to the fourfold symmetry axis of the electron pocket (e.g., along Γ - X). Transverse (\perp) refers to the cross section perpendicular to this axis, i.e., the W - X - U plane. The anisotropy in that plane between, say, X - W and X - U is negligible.

We now turn to a detailed comparison with the Fermi surface and Hall data on the Fermi-surface dimensions. The results are summarized in Tables II, III, and IV. We note first (see Table II) that our LDA calculated electron and hole concentrations of ErAs (corresponding to

TABLE II. Carrier concentrations and exchange splittings.

	$n_{e,h}$ (10^{20} cm $^{-3}$)	Δ_{xc}^{\perp} (meV)	Δ_{xc}^{\parallel} (meV)
ErAs (LDA)	9.0	80	157
ScAs (LDA)	9.5	0	0
Er $_x$ Sc $_{1-x}$ As (LDA)	8.7	48	65
Er $_x$ Sc $_{1-x}$ As (fit)	3.5	48	65
Er $_x$ Sc $_{1-x}$ As (expt.) ^a	3.2	47	

^aReference 4.

TABLE III. Shubnikov–de Haas frequencies f (in T).

Compound	$f_{h,l}$	$f_{h,h1}$	$f_{h,h2}$	$f_{e,\perp}^\uparrow$	$f_{e,\perp}^\downarrow$	$f_{e,\parallel}^\uparrow$	$f_{e,\parallel}^\downarrow$
Er As (LDA)	595	1808	1965	439	565	1925	2307
Sc As (LDA)	626	1643	1683	609	609	2104	2104
$\text{Er}_x\text{Sc}_{1-x}\text{As}$ (LDA)	456	1338	1406	479	555	1581	1811
$\text{Er}_x\text{Sc}_{1-x}\text{As}$ (fit)	281	885	925	327	397	1028	1236
$\text{Er}_x\text{Sc}_{1-x}\text{As}$ (expt.) ^a	153	941	941	324	386	1111	1247

^aReference 5. See text for assignment of peaks.

the total volume of the electron and hole Fermi-surface pockets) are about a factor of 3 larger than the observed ones for $\text{Er}_x\text{Sc}_{1-x}\text{As}$. Relatedly we find that our calculated SdH oscillation frequencies (Table III), which are directly proportional to the extremal cross-sectional areas of the Fermi surface perpendicular to the magnetic field, are significantly larger than the experimental ones. The question arises whether this is due to the Sc alloying or to the errors introduced by the LDA.

The LDA band structure of ScAs (at the ErAs lattice constant) differs slightly from that of ErAs. The Sc $3d$ -derived bands are shifted down towards the As-derived bands and have a smaller bandwidth. As a result, there is no Δ'_2 - Δ_5 crossing. Nevertheless, the Fermi-surface dimensions are even slightly larger than those of ErAs as can be seen in Tables II and III. Also, with the absence of an open $4f$ shell (in Sc) to induce it, there obviously is no spin splitting for ScAs.

The $\text{Er}_{0.6}\text{Sc}_{0.4}\text{As}$ band structure was modeled using a virtual-crystal approximation in which the Er $5d$ and Sc $3d$ and Er $6s(p)$ and Sc $4s(p)$ centers of the band parameters C_ℓ (Ref. 10) were arithmetically averaged and the corresponding bandwidth parameters Δ_ℓ were geometrically averaged. The spin splitting of the C_d parameter is appropriately reduced for the lower Er concentration. As can be seen in Table II, the magnitude and anisotropy of the exchange splitting are both significantly reduced by the alloying. However, the resulting Fermi-surface dimensions (Table III) and carrier concentrations (Table II) were not sufficiently reduced to explain the data.

We thus conclude that the LDA must be primarily responsible for the discrepancy in overall Fermi-surface dimensions. As is well known, the LDA is not directly applicable to the calculation of excitation energies (e.g., it underestimates semiconductor band gaps). Similarly, one may expect that quasiparticle self-energy corrections would shift the mainly Er $5d$ -derived conduction bands

upwards. This would raise the Δ'_2 band and thus reduce the Fermi volumes of both the electron and the hole pockets which should be equal in a semimetal. We thus introduced a semiempirical shift of the metal C_d potential parameter. It was found that a correction leading to a ~ 0.4 eV shift of the Δ'_2 band is needed to achieve agreement with the carrier concentrations obtained from the Hall data (see Table II). While this applies both for $\text{Er}_x\text{Sc}_{1-x}\text{As}$ and pure ErAs, only the former is further discussed here. The corrected $\text{Er}_{0.6}\text{Sc}_{0.4}\text{As}$ band structure is shown in Fig. 3.

The Fermi-surface dimensions for this band structure are in good agreement with all observed SdH frequencies as we now show. We note, however, that our assignment of the SdH frequencies differs from that of Bogaerts *et al.*⁵ Specifically, we find that the two heavy-hole surfaces have cross-sectional areas which are smaller than the longitudinal cross section of the ellipsoidal electron pocket. This result is insensitive to the LDA and alloy corrections. We thus assign the observed peak in the Fourier transform of the SdH oscillations at 941 T to the heavy holes and the observed peaks at 1111 and 1247 T to the exchange-split longitudinal cross section of the electron pocket, whereas Bogaerts *et al.*⁵ assigned the 941 T and 1111 T peaks to the electrons and the 1247 T peak to the holes. We note that our calculated cross-sectional areas for the two heavy-hole surfaces differ slightly (and both exhibit negligible exchange splitting). We assign the light-hole surface to a peak in the experimental data at ~ 153 T which previously has not been discussed by Bogaerts *et al.*⁵

The cyclotron mass is given by $m = (\hbar^2/2\pi)(\partial S/\partial E)_F$ where S_F is the area of the extremal cross section of the Fermi surface enclosed by the orbit in the plane normal to the magnetic field. The masses for B along [100] have been calculated for the three hole surfaces and for the electron pocket along the [100] ΓX axis (corresponding

TABLE IV. Cyclotron masses of light holes m_l , heavy holes m_{h1}, m_{h2} , and electrons $m_{e,\parallel}, m_{e,\perp}$ (in units of the free electron mass m_0).

Compound	$m_{h,l}$	$m_{h,h1}$	$m_{h,h2}$	$m_{e,\perp}$	$m_{e,\parallel}$
ErAs (LDA)	0.12	0.46	0.57	0.17	1.76
$\text{Er}_x\text{Sc}_{1-x}\text{As}$ (LDA)	0.11	0.42	0.42	0.16	1.33
$\text{Er}_x\text{Sc}_{1-x}\text{As}$ (fit)	0.11	0.37	0.38	0.16	1.19
$\text{Er}_x\text{Sc}_{1-x}\text{As}$ (expt.)		0.26 ^a	0.26 ^a	0.17 ^{a,b}	1.19 ^a

^aReference 5; see text for discussion.

^bReference 4.

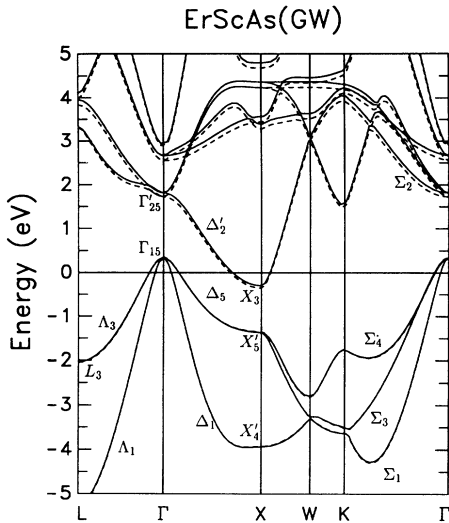


FIG. 3. Spin-polarized electronic band structure of $\text{Er}_{0.6}\text{Sc}_{0.4}\text{As}$ alloy in the virtual-crystal approximation with quasiparticle shift of the conduction band included. Solid and dashed curves as in Fig. 1.

to motion in a WXU plane) and are given as the first four entries in Table IV. From the cyclotron mass for one of the other electron pockets (corresponding to motion in a ΓKX plane) and the relation $m = (m_{e\parallel}m_{e\perp})^{1/2}$, relevant for an ellipsoidal surface, we determined $m_{e\parallel}$. Because the shape of the bands is relatively insensitive to the LDA and alloying corrections, the latter do not appreciably alter the masses, as is evident from Table IV. Good agreement is achieved for $m_{e\perp}$ which was determined experimentally by fitting the temperature and magnetic-field dependence of the SdH oscillations.⁴ The values given for $m_{e\parallel}$ and m_{HH} were determined by Bogaerts *et al.*⁵ Their value of $m_{e\parallel}$ however, should be changed to 1.57 if we reassign the SdH frequencies according to our interpretation. Their value for the hole mass involves a theoretical estimate⁷ of the Fermi level position with respect to the valence-band maximum. Comparing the latter with our calculation, their value of m_{HH} can be seen to be an underestimate.

We now compare our indicated 0.4 eV shift with an estimate of the quasiparticle self-energy correction. For this purpose, we use a simple scheme based on Hedin's so-called *GW* approximation¹⁶ and suggested by Bechstedt and Del Sole (BDS).¹⁷ In order to apply their approach to ErAs, we estimate the average dielectric constant $\bar{\epsilon} = 1 + (\hbar\omega_p/E_p)^2$, using the band gap at the

Baldereschi point^{18,19} as an estimate of the Penn gap E_p and where ω_p is the valence-electron plasmon frequency. We find that $E_p \approx 3.4$ eV and $\bar{\epsilon} \approx 22$. As in the BDS approach, we neglect the off-diagonal matrix elements of the self-energy correction operator between valence- and conduction-band states. The result is an estimated "gap" correction of 0.2 eV. Considering the crude nature of this estimate, this result is consistent with the value of 0.4 eV obtained from fitting the Fermi-surface dimensions.

Another origin of the self-energy correction may be hybridization of the states near the Fermi level with the 4*f* electrons, which was neglected here. However, preliminary estimates indicate that this effect is small because the Er 4*f* states lie at least 5 eV below the Fermi level.²⁰ Furthermore, the similarity between our results for ScAs and ErAs indicates that the 4*f* electrons are not the primary origin of the LDA overestimate of the carrier concentrations.

Finally, we note that according to Xia *et al.*'s analysis,⁷ the crossing of the Δ'_2 and Δ_5 bands inhibits the opening of a gap upon size quantization in thin [001] layers of RE-As buried in GaAs. The thermally activated behavior of the conductivity below 3 monolayers as observed by Allen *et al.*² was thus attributed to the lack of a continuous film below 3 monolayers instead of a genuine metal-semiconductor transition. Since we find that the "corrected" band structure does not have this crossing, we believe that this question is worth reexamining experimentally.

In conclusion, we have presented spin-polarized band-structure and total energy calculations of ErAs and have made a detailed comparison with experimental data on the Fermi-surface dimensions and exchange splittings of the related $\text{Er}_x\text{Sc}_{1-x}\text{As}$ alloy. Good agreement with the experimentally determined Fermi-surface dimensions was obtained only when a quasiparticle self-energy correction similar to the gap correction in semiconductors was introduced. On the basis of our calculations, we propose a different assignment of the observed SdH frequencies than that proposed by Bogaerts *et al.*⁵ The magnetic exchange splittings, which are strongly anisotropic in pure ErAs, but less so in $\text{Er}_x\text{Sc}_{1-x}\text{As}$, and the cyclotron masses were found to be in good agreement with the data irrespective of the corrections to the LDA.

This work was supported by ONR Grant No. N00014-93-10425. We thank Max. N. Yoder for stimulating our interest in the rare-earth compounds and C. J. Palmstrøm, S. J. Allen, Jr., and R. Bogaerts for useful discussions.

¹C. J. Palmstrøm, N. Tabatabaie, and S. J. Allen, Jr., *Appl. Phys. Lett.* **53**, 2608 (1988).

²S. J. Allen, D. Brehmer, and C. J. Palmstrøm, in *Rare Earth Doped Semiconductors*, edited by G. S. Pomrenke, P. B. Klein, and D. W. Langer, MRS Symposia Proceedings No. 301 (Materials Research Society, Pittsburgh, 1993), p. 307.

³F. Hulliger, in *Handbook on the Physics and Chemistry of Rare Earths*, edited by K. A. Gshneidner and L. Eyring (North-Holland, Amsterdam, 1979), Vol. 4, p.153.

⁴S. J. Allen, Jr., N. Tabatabaie, C. J. Palmstrøm, G. W. Hull, T. Sands, F. DeRosa, and H. L. Gilchrist, *Phys. Rev. Lett.* **62**, 2309 (1989); S. J. Allen, Jr., F. DeRosa, C. J. Palmstrøm, and A. Zrenner, *Phys. Rev. B* **43**, 9599 (1991).

⁵R. Bogaerts, L. Van Bockstal, F. Herlach, F. M. Peeters, F. DeRosa, C. J. Palmstrøm, and S. J. Allen, Jr., *Physica B* **177**, 425 (1992); **184**, 2320 (1993).

⁶A. Hasegawa and A. Yanase, *J. Phys. Soc. Jpn.* **42**, 492 (1977).

- ⁷Jian-Bai Xia, Shang-Fen Ren, and Yia-Cung Chang, Phys. Rev. B **43**, 1692 (1991).
- ⁸P. Hohenberg and W. Kohn, Phys. Rev. **136**, B864 (1964); W. Kohn and L. J. Sham, *ibid.* **140**, A1133 (1965).
- ⁹U. von Barth and L. Hedin, J. Phys. C **5**, 1629 (1972).
- ¹⁰O. K. Andersen, O. Jepsen, and M. Šob, in *Electronic Band Structure and its Applications*, edited by M. Yussouff (Springer, Heidelberg, 1987).
- ¹¹The Er $5p$ semicore band dispersion is taken into account. Er $6p$ states lie at 2.5 Ry above the Fermi level and were neglected in the total energy calculations and in Fig. 1. They were included in the basis set for the virtual-crystal Er_xSc_{1-x}As alloy.
- ¹²When Er $4f$ was treated in a single-particle band picture, a narrow Er $4f$ -derived band appeared at the Fermi level, which is not in agreement with the observed semimetallic nature of the compound.
- ¹³P. H. Dederichs, S. Blügel, R. Zeller, and H. Akai, Phys. Rev. Lett. **53**, 2512 (1984).
- ¹⁴M. S. S. Brooks, L. Nordström, and B. Johansson, J. Phys. Condens. Matter **3**, 2357 (1991).
- ¹⁵Tōru Moriya, J. Magn. Magn. Mater. **14**, 1 (1979).
- ¹⁶L. Hedin, Phys. Rev. **139**, A796 (1965); L. Hedin and S. Lundqvist, in *Solid State Physics: Advances in Research and Applications*, edited by F. Seitz, D. Turnbull, and H. Ehrenreich (Academic, New York, 1969), Vol. 23, p. 1.
- ¹⁷F. Bechstedt and R. del Sole, Phys. Rev. B **38**, 7710 (1988).
- ¹⁸A. Baldereschi, Phys. Rev. B **7**, 5212 (1973).
- ¹⁹M. Cardona and N. E. Christensen, Phys. Rev. B **35**, 6182 (1987).
- ²⁰J. K. Lang, Y. Baer, and P. A. Cox, J. Phys. F **11**, 121 (1981).